Electronic Supplementary Material (ESI) for Journal of Materials Chemistry A.

Tailored Imidazolium Tetraphenylborate Salts for the Design of Boron, Nitrogen co-Doped Carbon Materials as High-Performance Anodes for Fast-Rate Monovalent Ion Batteries

Soha Aldroubi,[a] Badre Larhrib,[a,b] Louiza Larbi,[a,c] Ibrahim Bou Malham,[d] Camelia Matei Ghimbeu [c, e], Laure Monconduit,[a,e] Ahmad Mehdi[a,*] and Nicolas Brun[a,*]

[a.] *ICGM, Univ. Montpellier, CNRS, ENSCM, Montpellier, France.*
[b.] *Université de Pau, Avenue de l'Université, 64012 Pau Cedex.*
[c.] *Institut de Science des Matériaux de Mulhouse, IS2M, CNRS UMR 7361, UHA.*
[d.] *Laboratoire Energétique et Réactivité à l'Echelle Nanométrique (EREN), Faculté des Sciences IV, Université Libanaise, Haouch el-Omara, 1801 Zahlé, Liban.*
[e.] *RS2E, CNRS, Amiens, France.*

Synthesis of 1-benzyl-3-methylimidazolium chloride [(Bn)mim]Cl

1-benzyl-3-methylimidazolium chloride was obtained by preparing a mixture containing 1-methylimidazole (24.1 g, 0.294 mol) with benzyl chloride (41.0 g, 0.323 mol; which corresponds to a 1:1.1 molar ratio; see reaction (1) below) in 100 mL of acetonitrile under reflux at 80 °C for 3 hours and by stirring for 24 hours at room temperature.

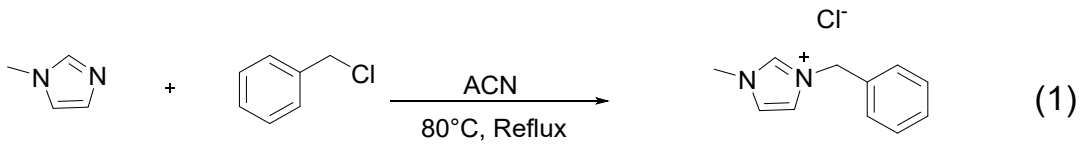

(1)

Fig. S1. Synthesis of 1-benzyl-3-methylimidazolium chloride (1).

Hexane (3 × 50 mL) was used to remove the excess of benzyl chloride. After washing, the acetonitrile was removed *via* rotary evaporation. The as-synthesized viscous IL was freeze-dried overnight.

[(Bn)mim]Cl: (58.2 g, 0.279 mol). Yield: 95%. **^{1}H NMR (400 MHz, $CDCl_3$)** δ 10.64 (s, 1H) ; 7.67-7.29 (m, 7H) ; 5.52 (s, 2H) ; 3.99 (s, 3H). **^{13}C NMR (126 MHz,$CDCl_3$)** δ 137.67; 133.26; 129.35; 129.32; 128.85; 123.8; 121.92; 53.12; 36.53. **Elemental analysis**. wt% theoretical: C (63.309); H (6.278); N (13.422). wt% analytical: C (61.929); H (6.235); N (13.062).

Synthesis of 1,3-(benzyl)imidazolium chloride [$(Bn)_2$im]Cl

1,3-bis(benzyl)imidazolium chloride was synthesized by dissolving sodium hydride (6.6 g, 0.164 mol) in 50 mL of THF in a three-necked flask placed in an ice bath and equipped with a condenser. *Safety precaution: NaH can ignite spontaneously in air and reacts vigorously with water, releasing hydrogen (flammable) and sodium hydroxide (caustic base).* An equimolar amount of imidazole (11.3 g, 0.164 mol) dissolved in 100 mL of this same solvent was gradually added to the mixture, which was stirred continuously using a magnetic stirrer. Once the addition was completed, the ice bath was removed (see reaction (3)). Benzyl chloride (42.0 g, 0.328 mol) was poured into the reaction medium in a 2:1 molar ratio relative to the imidazole. Stirring at room temperature was maintained for 12 hours. The sodium chloride was eliminated by filtration on sintered glass topped with celite (reactions (4) and (5)). Washing with hexane (3×50 mL) was carried out to remove traces of benzyl chloride. THF was removed by rotary evaporation. Finally, the ionic liquid was freeze-dried.

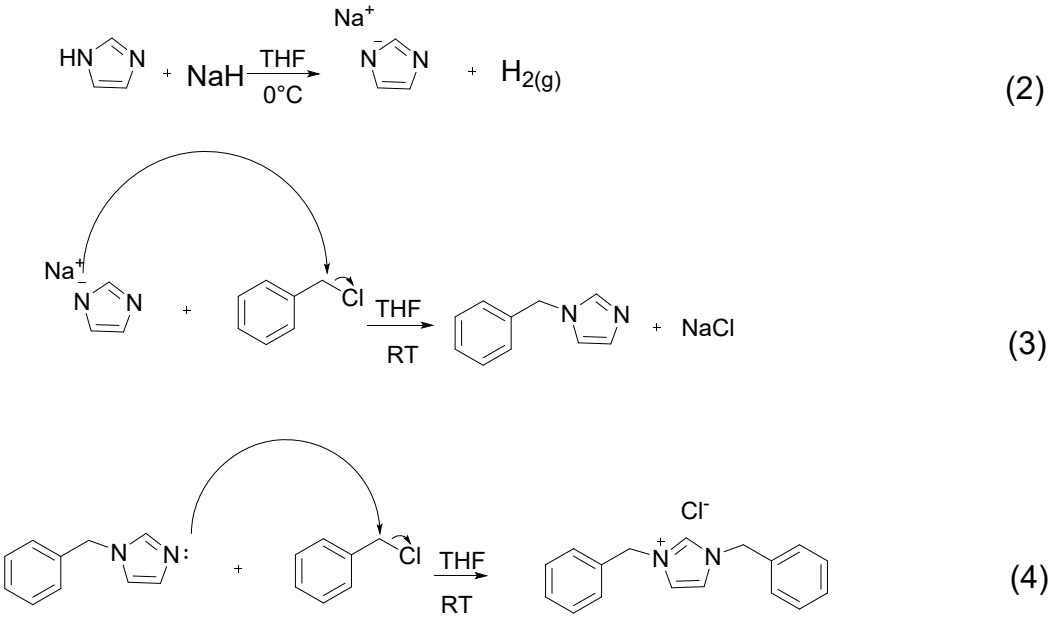

Fig. S2. Synthesis of 1,3-bis(benzyl)imidazolium chloride (4).

[$(Bn)_2$im]Cl: (29.43 g, 0,103 mol). Yield : 63%. **^{1}H NMR (400 MHz, $CDCl_3$)** δ 11.25 (s, 1H); 7.84-6.87 (m, 12H); 5.57 (s, 4H). **^{13}C NMR (126 MHz, $CDCl_3$)** δ 138.08; 132.82; 129.57; 129.50; 129.03; 121.59; 53.54. **Elemental analysis.** wt% theoretical: C (71.697); H (6.016); N (9.836). wt% analytical: C (70.685); H (6.248); N (9.391).

Synthesis of 1-butyl-3-methylimidazolium bromide [Bmim]Br

1-Butyl-3-methylimidazolium bromide is obtained from the reaction between 1-methylimidazole (17.5 g, 0.214 mol) and 1-bromobutane (30.4 g, 0.220 mol) in a molar ratio 1:1.1 in 100 mL of ethyl acetate under heating under reflux for 12 hours. Two phases are formed: a lower phase containing the ionic liquid and an upper phase consisting of ethyl acetate which dissolves what remains of the 1-methylimidazole and 1-bromobutane. Washing of the [Bmim][Br] with ethyl acetate under reflux repeated at least 3 times (3×50mL) and elimination of the upper phase are carried out each time. An

elimination of the remaining ethyl acetate via a rotary evaporator and a freeze-drying of the [Bmim][Br] (43.1 g, 0.197 mol) is carried out at the end. Yield: 92%.

Characterizations of the three imidazolium tetraphenylborate salts

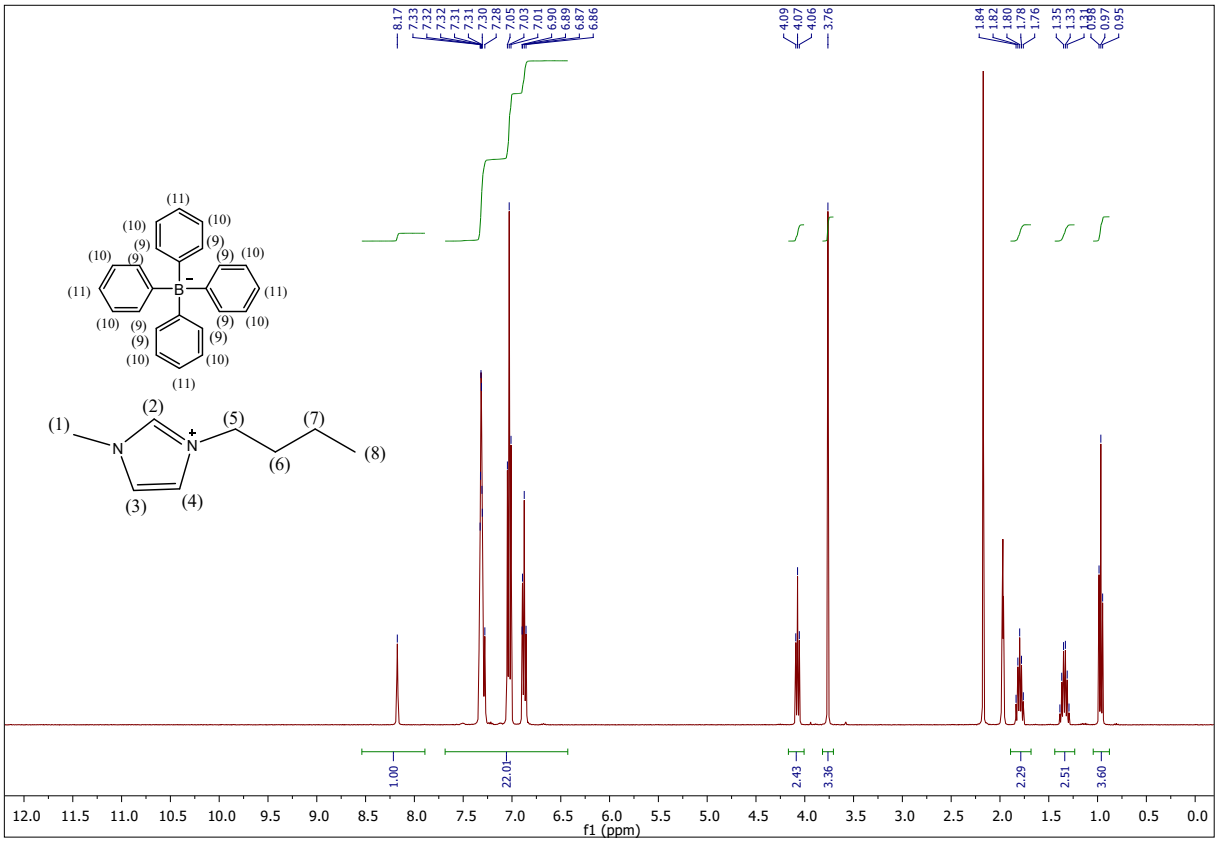

Figure S3. ^{1}H NMR [Bmim][BPh_4] (400 MHz, CD_3CN) δ 8.17 (s, 1H, (2)) ; 7.69-6.43 (m, 22H, (2), (3), (9), (10), (11)) ; 4.07 (t, 2H, (5)) ; 3.76 (s, 3H, (1)) ; 1.91-1.68 (m, 2H, (6)) ; 1.48-1.23 (m, 2H, (7)) ; 0.97 (t, 3H, (8)).

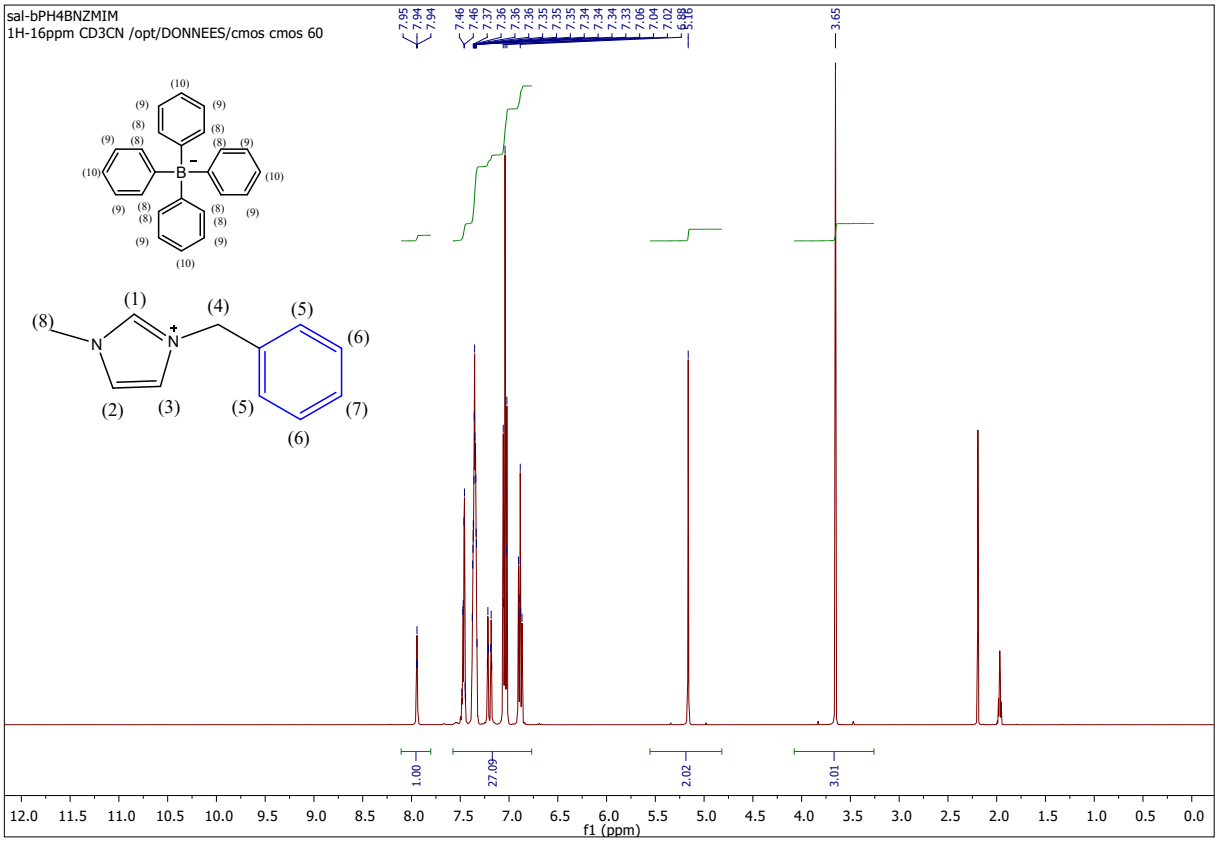

Figure S4. ^{1}H NMR [(Bn)mim][BPh_4] (400 MHz, CD_3CN) δ 7.94 (s, 1H, (1)) ; 7.61-6.77 (m, 27H, (2), (3), (5), (6), (7), (10), (9), (8)) ; 5.16 (s, 2H, (4)) ; 3.65 (s, 3H, (8)).

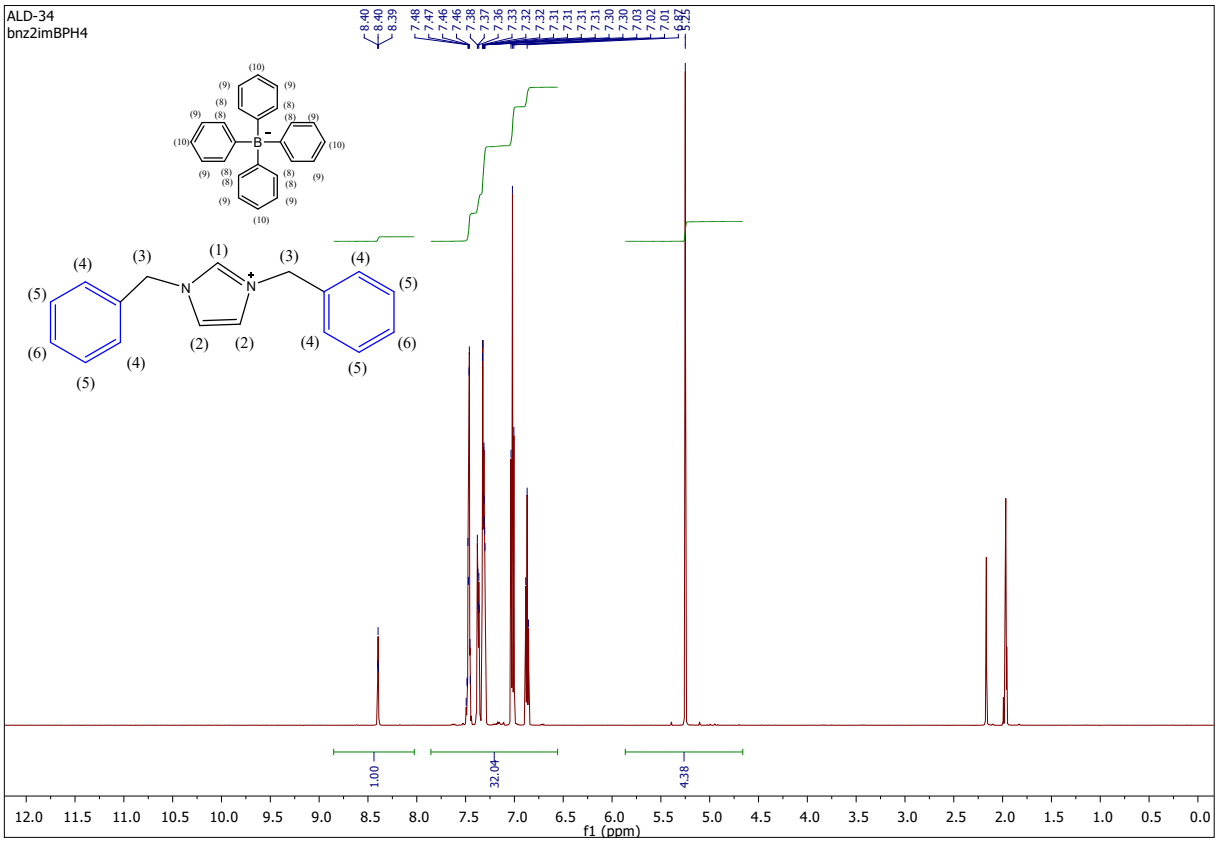

Figure S5. ^{1}H NMR $[(Bn)_2im][BPh_4]$ (400 MHz, CD_3CN) δ 8.40 (s, 1H, (1)) ; 7.89-6.57 (m, 32H, (2) , (4), (5), (6)) ; 5.25 (s, 4H, (3)).

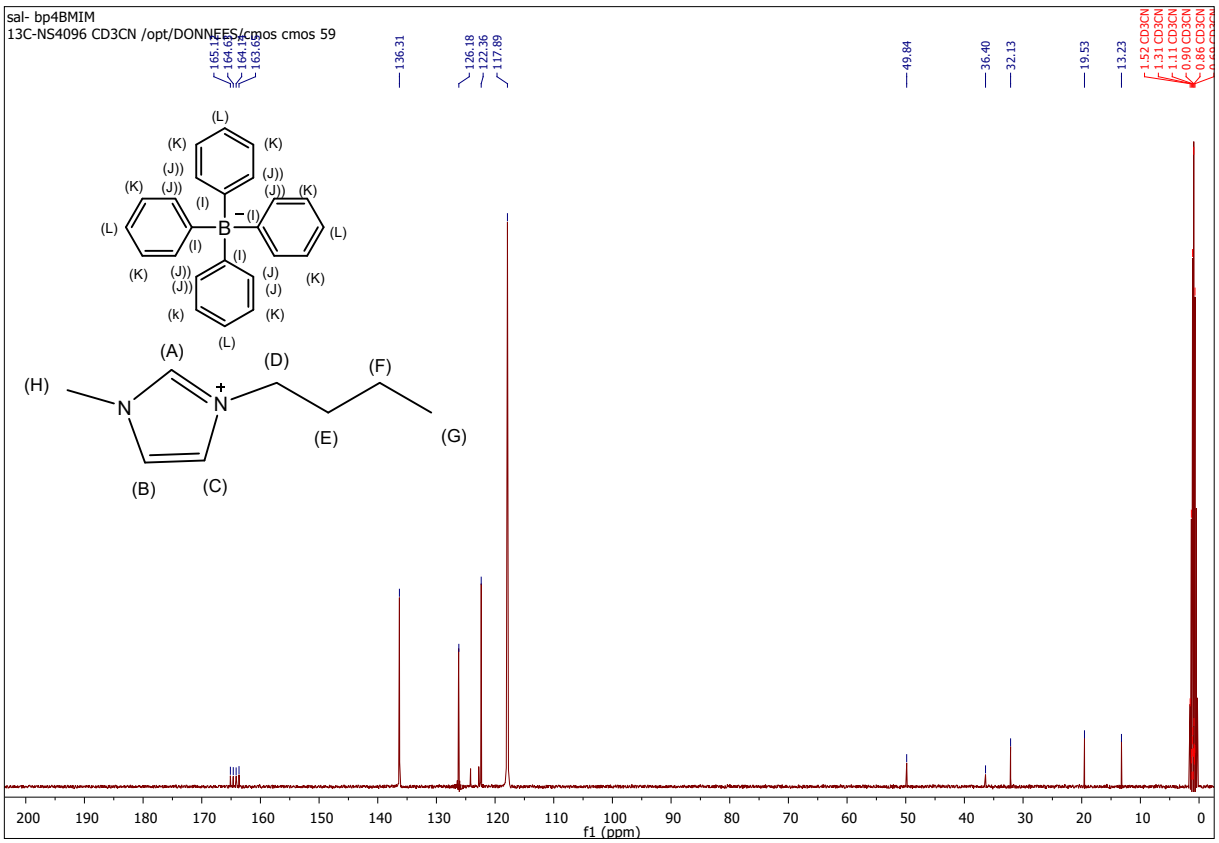

Fig. S6. ^{13}C NMR [Bmim][BPh_4] (101 MHz, CD_3CN) δ 165.12-163.65 ((I), (J), (K), (L)) ; 136.31 (A) ; 126.18 (C) ; 122.36 (B) ; 49.84 (D) ; 36.40 (H) ; 32.13 (E) ; 19.53 (F) ; 13.23 (G).

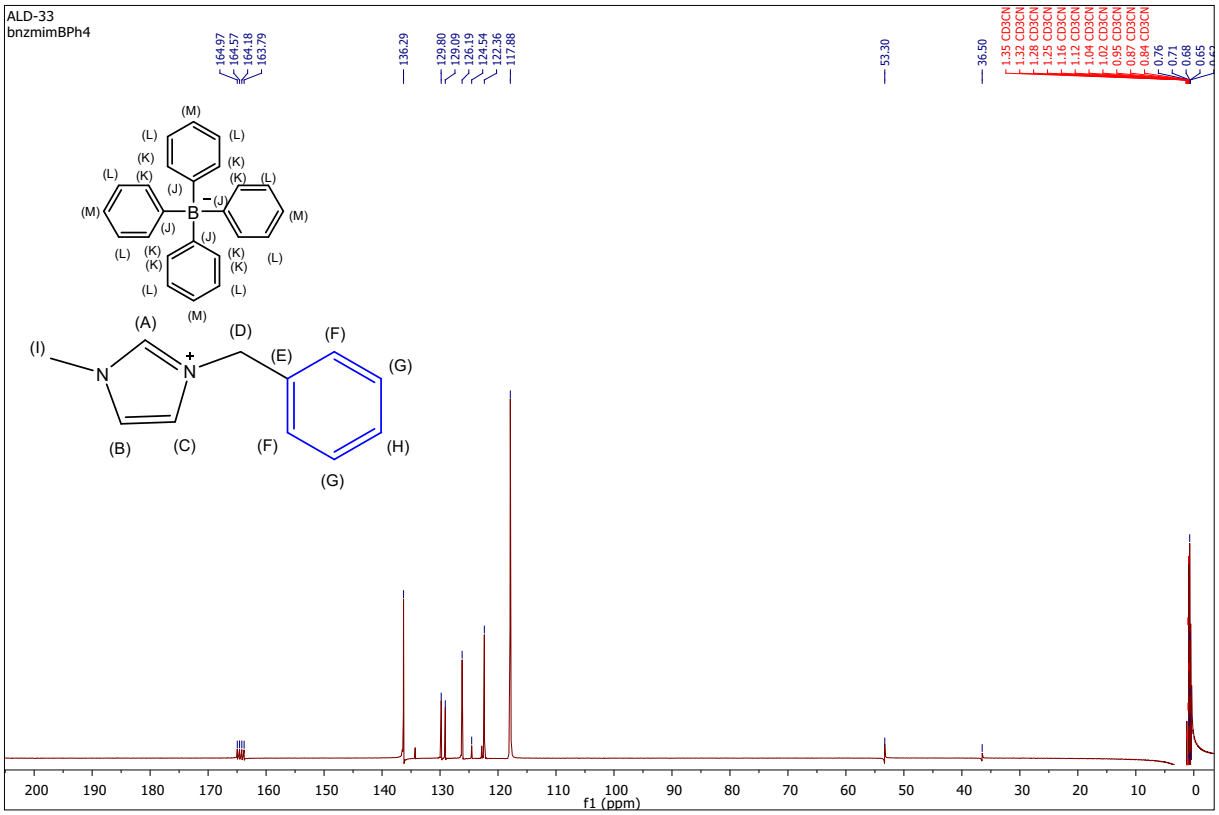

Fig. S7. ^{13}C NMR [(Bn)mim][BPh_4] (126 MHz, CD_3CN) δ 164.79-163.79((J), (K), (L), (M)) ; 136.29 (A) ; 129.80 (E) ; 129.09 (F) ; 126.19 (G) ; 124.54 (H) ; 122.36 ((C), (B)) ; 53.30 (D) ; 36.50 (I).

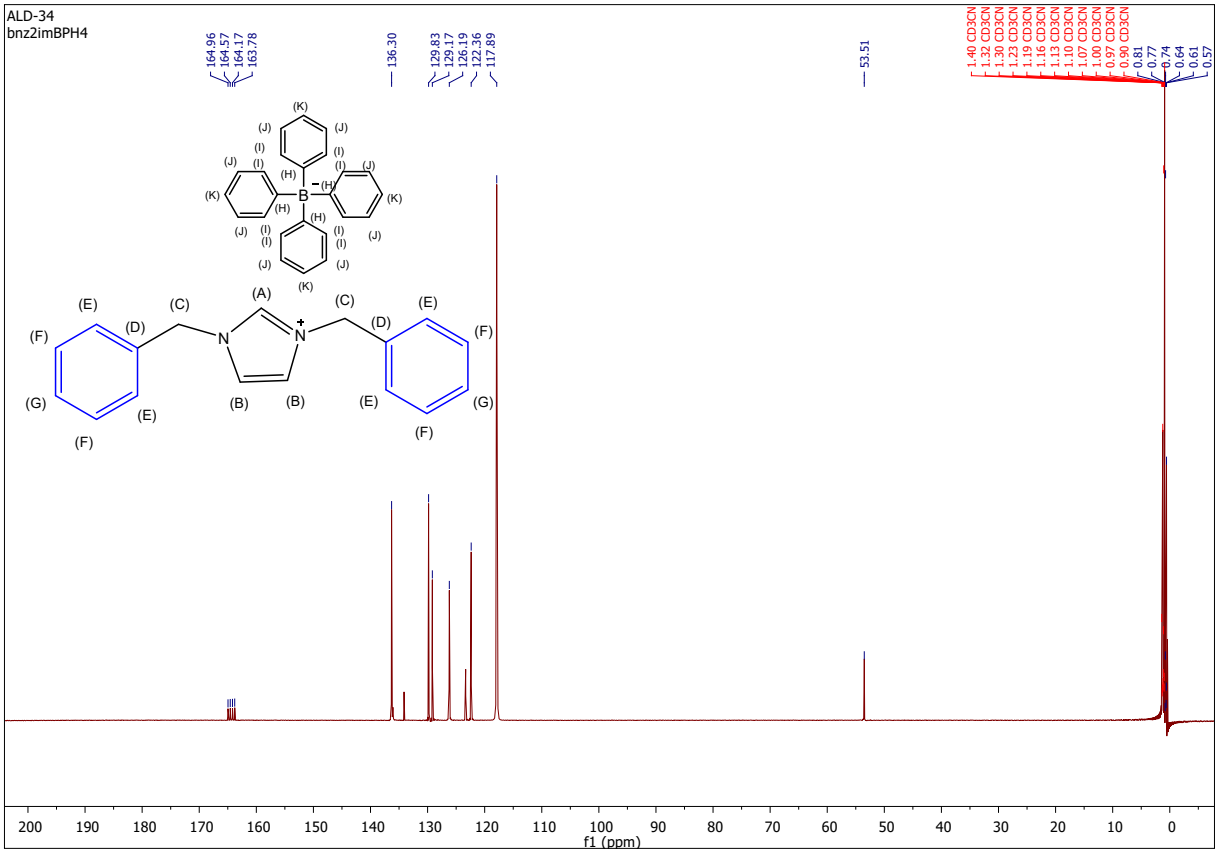

Fig. S8. ^{13}C NMR [$(Bn)_2im$][BPh_4] (126 MHz, CD_3CN) δ 168.37-160.78 ((H), (I), (J), (K)) ; 136.30 (A) ; 129.83 (D) ; 129.17 (E) ; 126.19 (F) ; 122.36 (G) ; 117.89 (K) ; 53.51 (C).

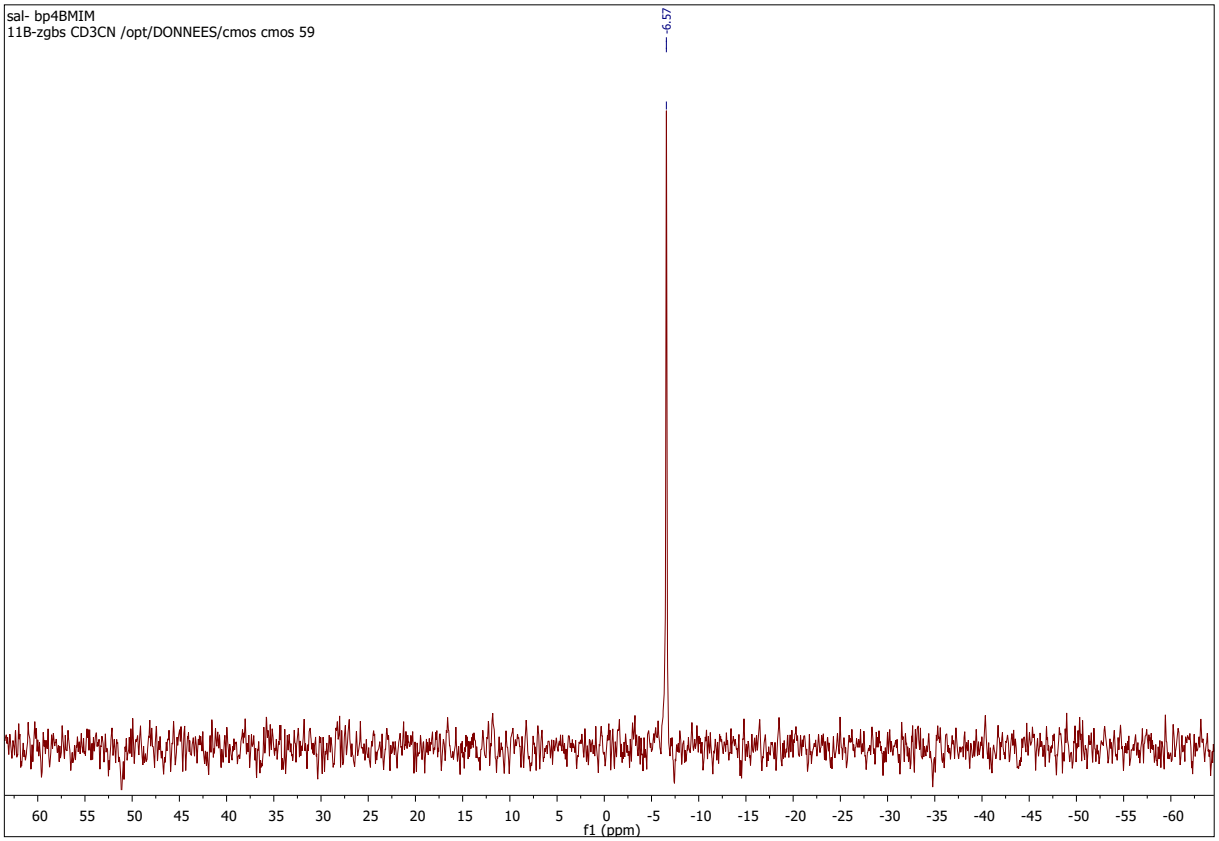

Fig. S9. ^{11}B NMR [Bmim][BPh_4] (128 MHz, CD_3CN) δ -6.57.

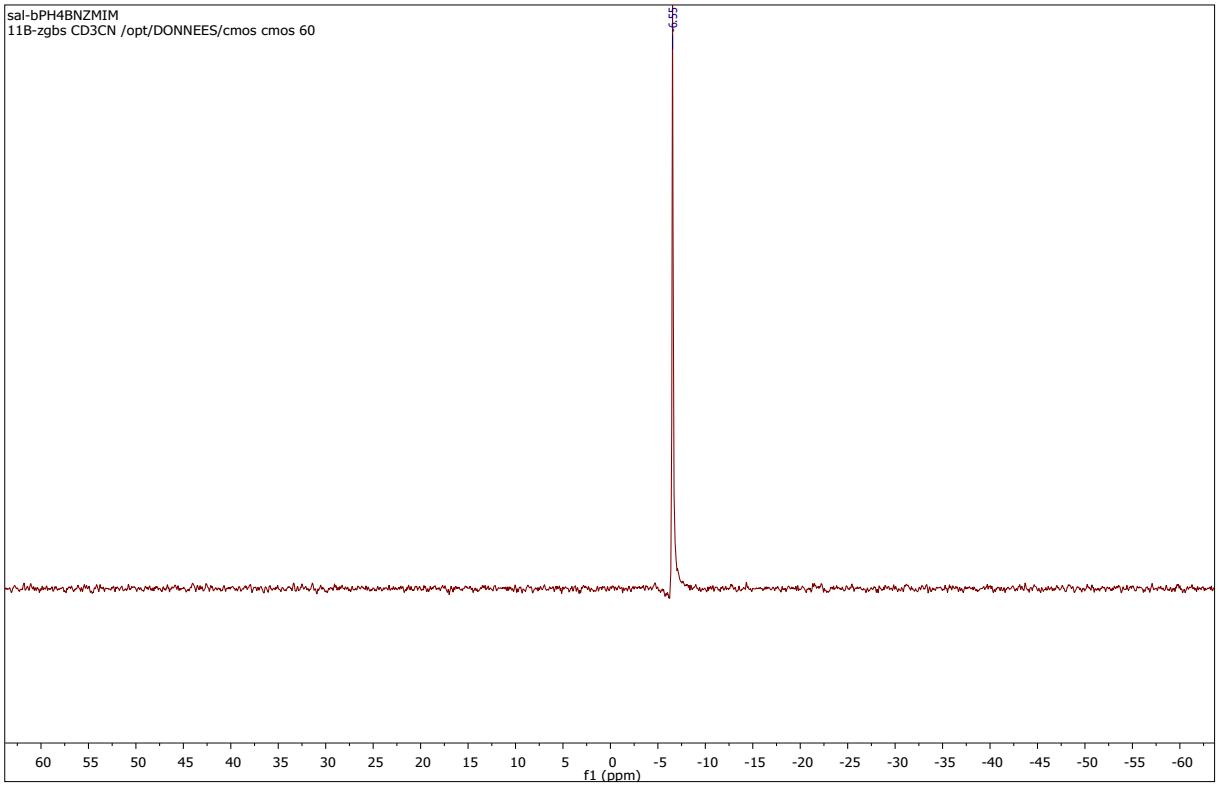

Fig. S10. ^{11}B NMR [(Bn)mim][BPh_4] (128 MHz, CD_3CN) δ -6.55.

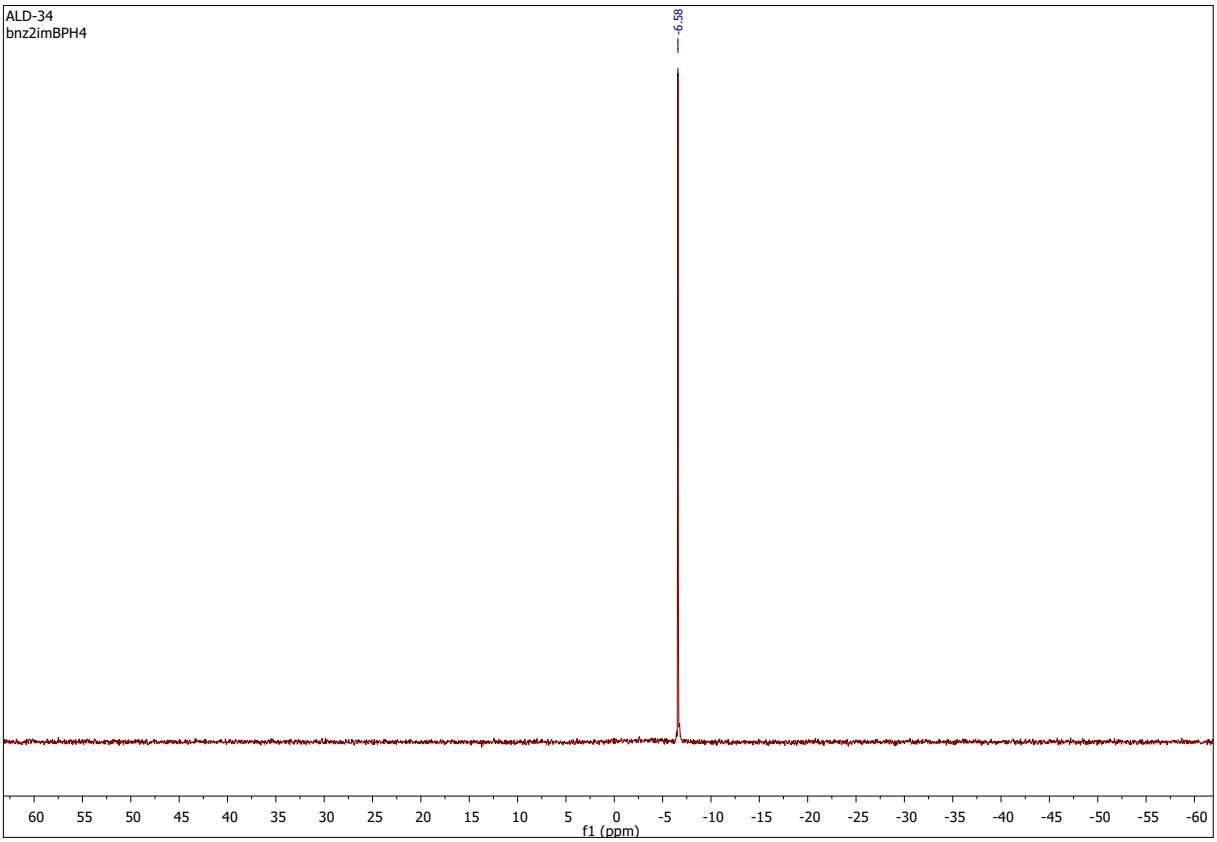

Fig. S11. ^{11}B NMR $[(Bn)_2im][BPh_4]$ (160 MHz, CD_3CN) δ -6.58.

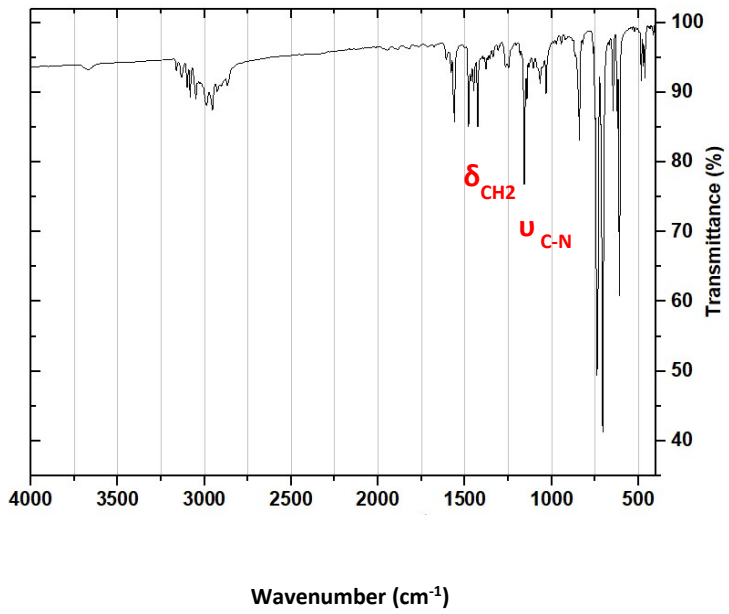

$\nu_{=CH}$ 3080-3030 cm^{-1} $\upsilon_{=CH}$ $\upsilon_{CH3, CH2}$ $\upsilon_{C=N}$ $\upsilon_{C=C}$

ν_{CH_3, CH_2} 2850-2960 cm^{-1}

$\nu_{C=N}$ 1690-1640 cm^{-1}

$\nu_{C=C}$ 1500, 1450 cm^{-1}

δ_{CH_2} 1485-1445 cm^{-1}

ν_{C-N} 1360-1310 cm^{-1}

Fig. S12. FTIR spectrum of [Bmim][BPh_4].

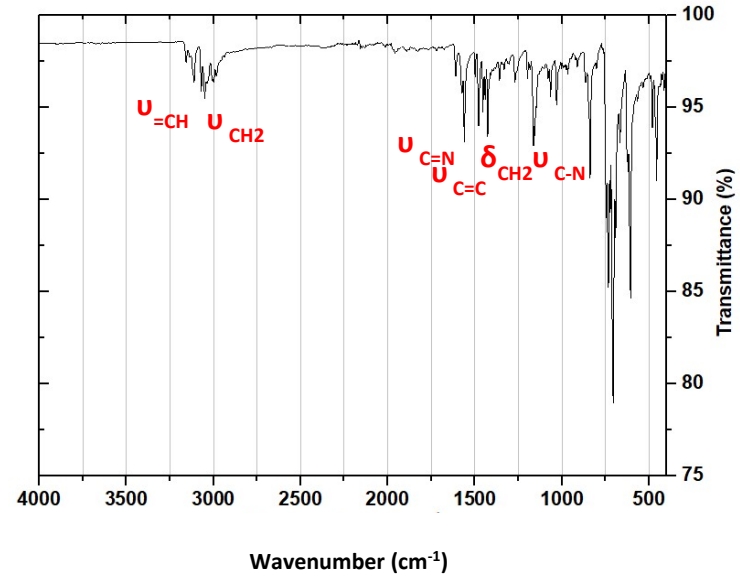

$\nu_{=CH}$ 3080-3030 cm^{-1}

ν_{CH_3, CH_2} 2850-2960 cm^{-1}

$\nu_{C=N}$ 1690-1640 cm^{-1}

$\nu_{C=C}$ 1500, 1450 cm^{-1}

δ_{CH_2} 1485-1445 cm^{-1}

ν_{C-N} 1360-1310 cm^{-1}

Fig. S13. FTIR spectrum of [(Bn)mim][BPh_4].

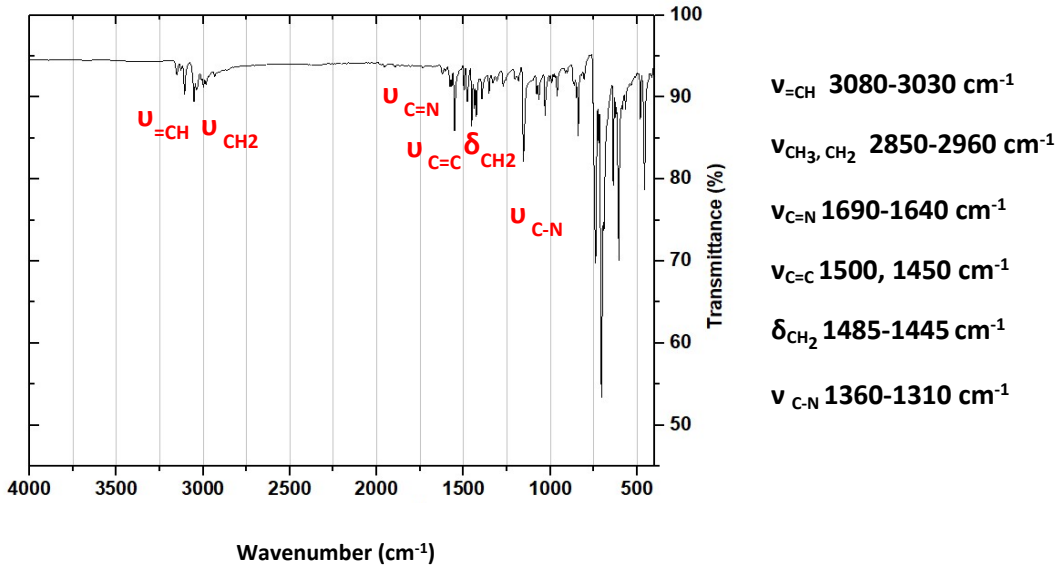

Fig. S14. FTIR spectrum of $[(Bn)_2im][BPh_4]$.

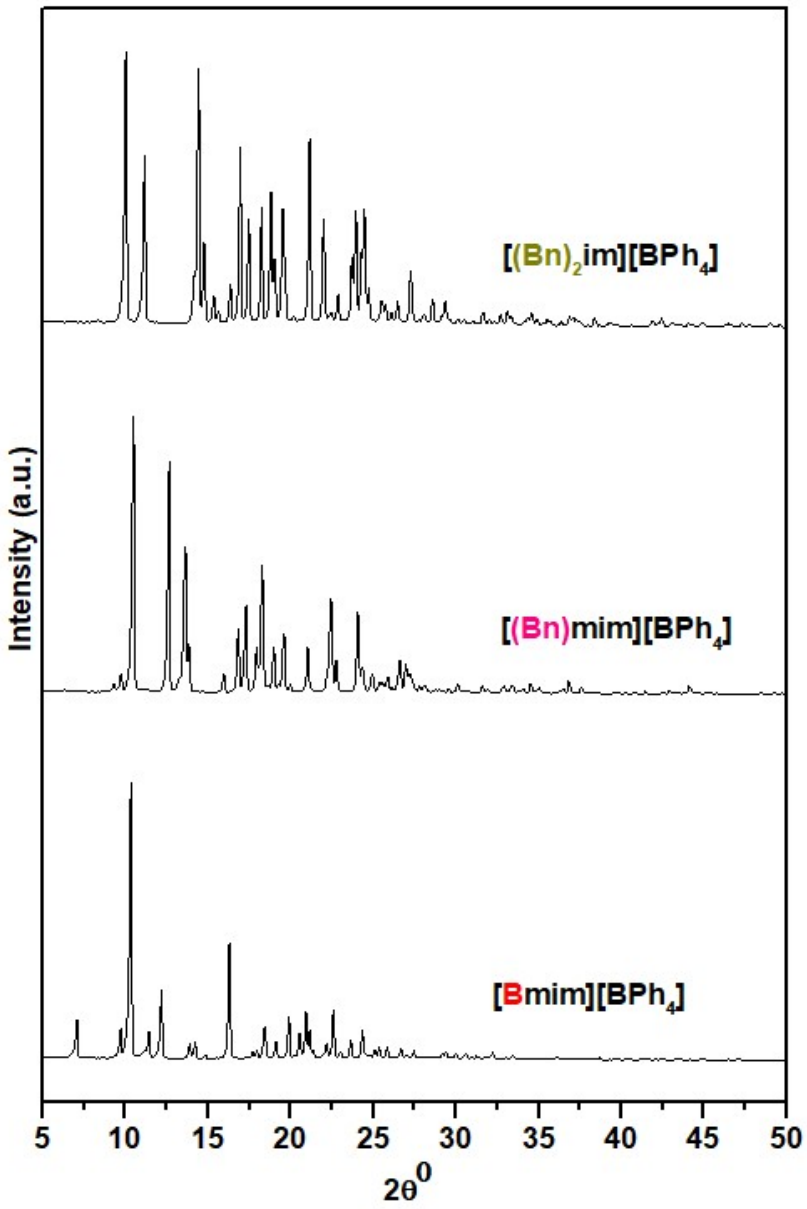

Figure S15. XRD diffractograms of [Bmim][BPh_4], [(Bn)mim][BPh_4] and [$(Bn)_2$im][BPh_4] salts.

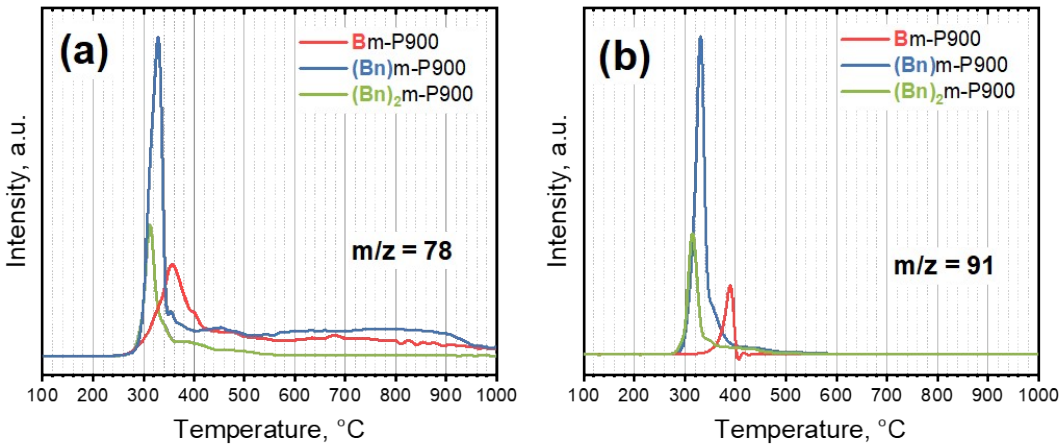

Figure S16. TG-MS curves showing the two most prominent masses, *i.e.*, m/z = (a) 78 and (b) 91, for the three imidazolium tetraphenylborate salts obtained under argon between 25 and 1100°C with a rate of 10°C/min.

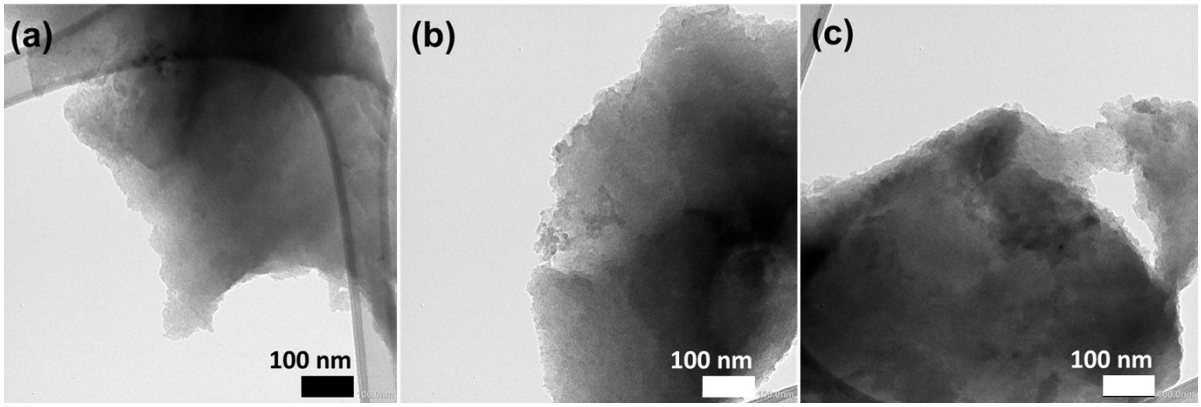

Figure S17. TEM micrographs of (a) Bm-P900, (b) (Bn)m-P900, and (c) $(Bn)_2$-P900.

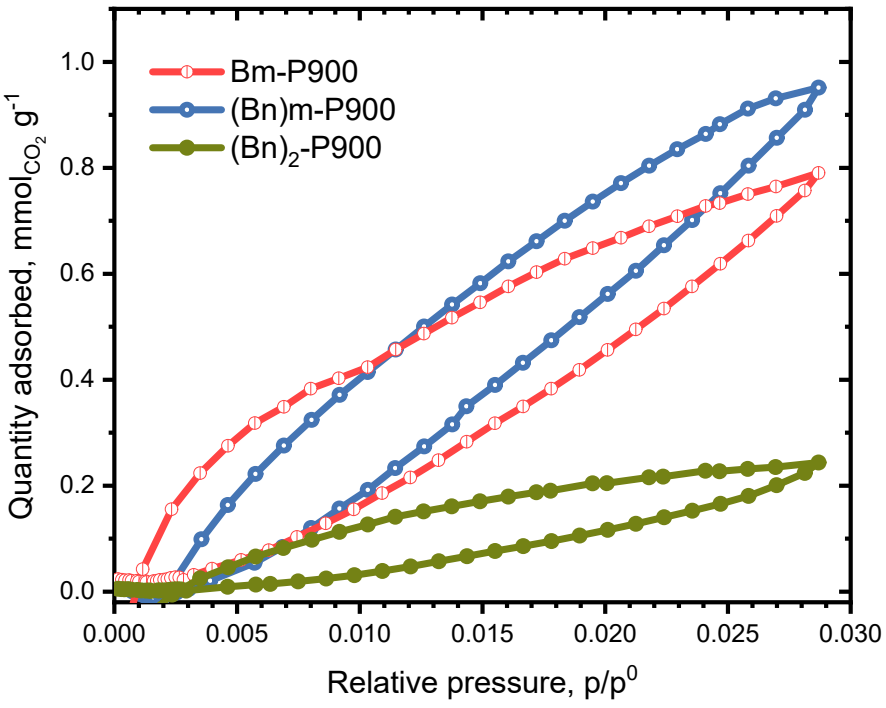

Figure S18. Carbon dioxide sorption isotherms at 273 K of Bm-P900, (Bn)m-P900, and $(Bn)_2$-P900.

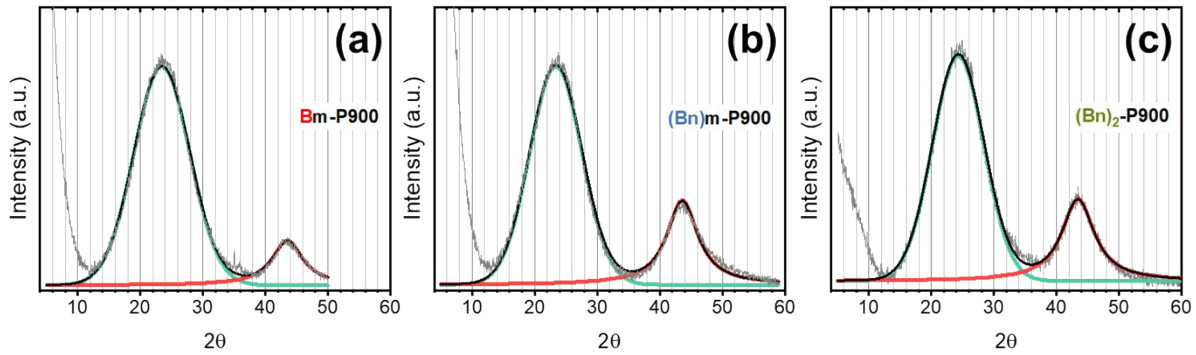

Fig. S19. X-ray diffraction profiles after fitting of **(a)** Bm-P900, **(b)** (Bn)m-P900 and **(c)** $(Bn)_2$-P900.

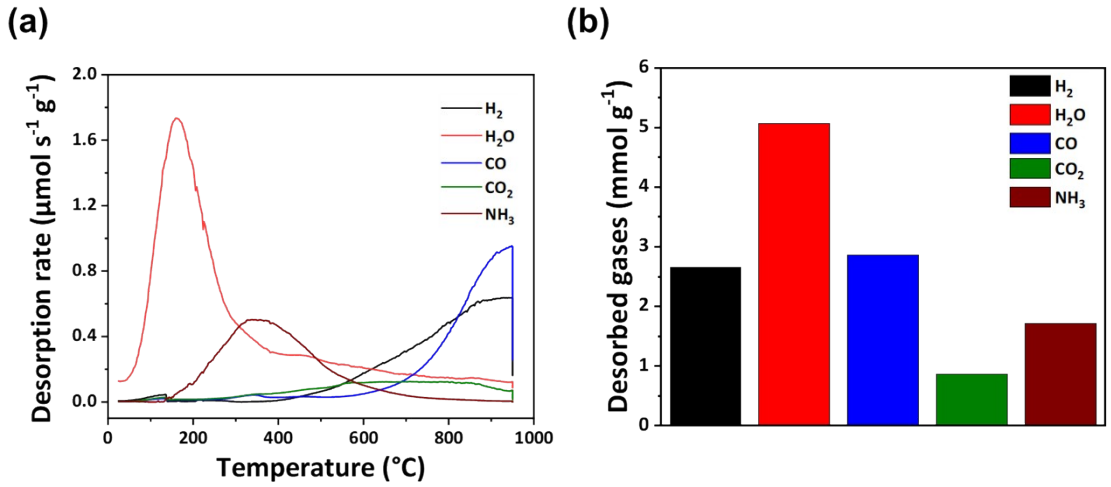

Figure S20. (a) TPD-MS profile of the desorbed gases during heating under vacuum and **(b)** the desorbed quantities of gases for $(Bn)_2$-P900.

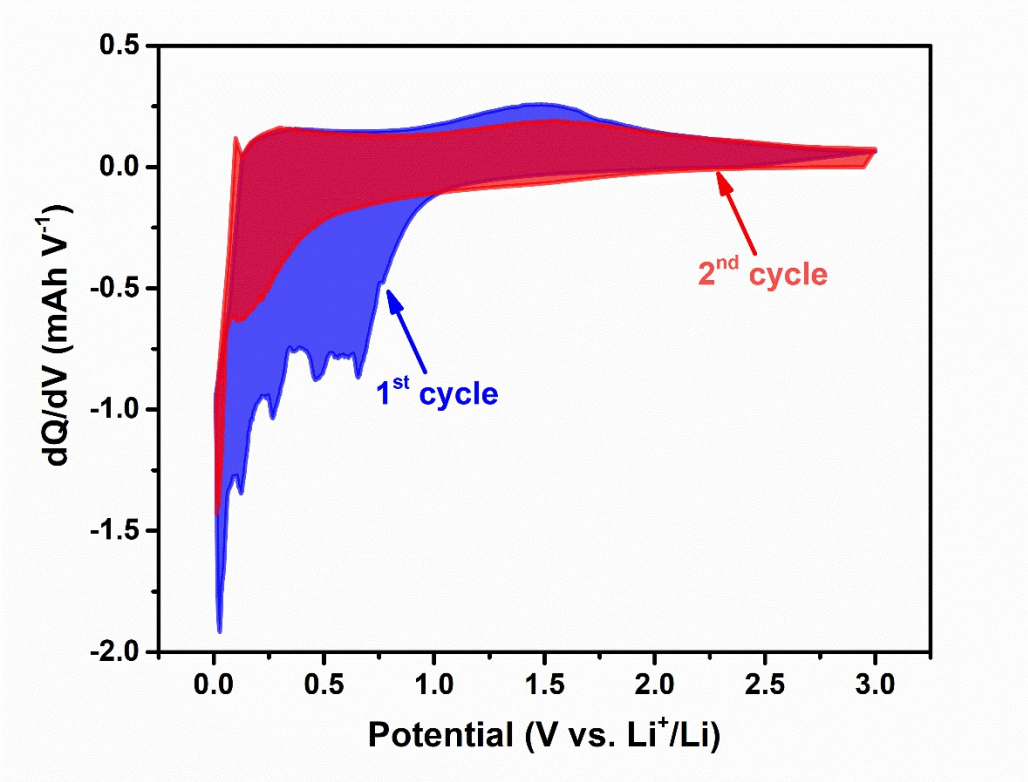

Fig. S21. 1st and 2nd differential capacity dQ/dV profiles of $(Bn)_2$-P900.

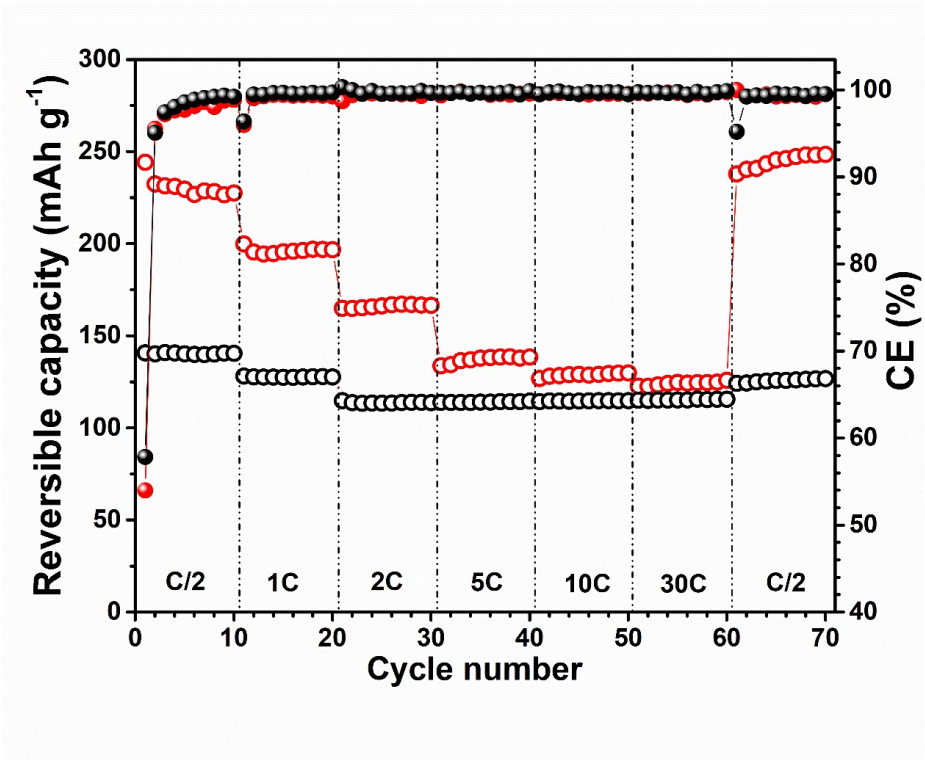

Figure S22. Rate performance and coulombic efficiency obtained between 3 and 0.01 V for $(Bn)_2$-P900 (red) and $(Bn)_2$-Cl-P900 (black).

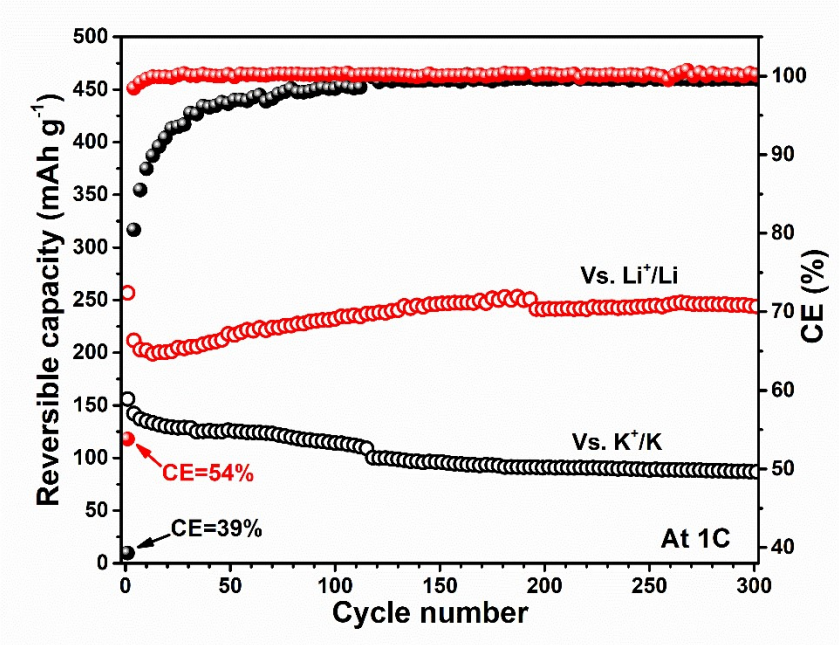

Fig. S23. Rate performance and coulombic efficiency upon 30 cycles at 1C obtained between 3 and 0.01 V for N-B doped Carbon versus Li and K.

Table S1. XPS peaks' attribution of carbon materials $(Bn)_2$-P900, (Bn)m-P900 and Bm-P900.

	Attribution	Position (eV)	FWHM (eV)	at.% $(Bn)_2$-P900	at.% (Bn)m-P900	at.% Bm-P900
C 1s	C-B	283.6	0.9	2.4	2.1	2.2
	C=C	284.3	0.9	45.9	39.2	31.0
	C-C/C-H	284.9	1.3	22.8	32.8	35.7
	C-O/C-N	286.1	1.6	7.8	5.6	7.2
	O-C=O/N-C=O	287.7	1.6	1.6	1.5	1.0
	Pi Pi*	289.8	3.0	4.9	5.8	2.4
O 1s	O-C=O/N-C=O	530.1	1.3	1.8	2.0	1.4
	C-O/C-N	531.9	1.6	6.4	5.1	6.0
	B-O	533.1	1.8	0.6	0.7	2.8
B 1s	C-B	188.7	1.8	2.4	2.1	2.2
	C-B-N	190.2	1.9	0.5	0.3	0.4
	BN/BC_2O	191.7	1.8	0.6	0.2	0.4
	B-O	193.0	1.7	0.6	0.6	2.8
N 1s	Pyridinic-N	398.4	1.8	0.5	0.5	2.0
	Pyrrolic-N	399.6	1.7	0.8	0.4	0.6
	Graphitic-N	400.6	1.7	0.2	1.0	2.0
	NOx	402.8	1.8	0.1	0.2	0.2

Table S3. Comparison of the electrochemical performance of various boron and nitrogen doped carbon-based anode materials. AM: Active material; CB: carbon black; PVDF: polyvinylidene difluoride

Table S2. Fitting results for the Raman spectra of the three carbon materials $(Bn)_2$-P900, (Bn)m-P900 and Bm-P900.

Sample	Function	Attribution	FWHM (cm^{-1})	Max height (a.u.)	Position at max height (cm^{-1})	Integrated area (%)
Bm-P900	Lorentz	D	190	795	1358	55
	Lorentz	G	75	534	1580	16
	Lorentz	D’	52	245	1620	5
	Gaussian	D”	126	313	1500	11
	Lorentz	I	170	209	1210	13
(Bn)m-P900	Lorentz	D	192	1432	1365	55.5
	Lorentz	G	81	974	1584	17
	Lorentz	D’	59	645	1620	8.5
	Gaussian	D”	124	507	1500	10
	Lorentz	I	155	289	1210	9
$(Bn)_2$-P900	Lorentz	D	187	1087	1365	56
	Lorentz	G	83	766	1586	19
	Lorentz	D’	59	445	1622	8
	Gaussian	D”	126	389	1500	10
	Lorentz	I	197	197	1210	7

Material	Electrode formulation	Electrolyte	Capacity (mAh g^{-1}) / iCE / low rate (mA g^{-1}) / capacity retention	Capacity (mAh g^{-1}) at high C-rate (mA g^{-1})	Ref
Nitrogen and sulfur dual-doped graphene sheets (NSGs-3)	80:10:10 AM:acetylene black:PVDF	1 M $LiPF_6$ (EC/DMC)	593 / 59% / 100 / 82% after 500 cycles	107 at 5000	1
N-doped graphene B-doped graphene	70:15:15 AM:Acetylene black:PVDF	1M $LiPF_6$ (EC/DEC)	1443 / 49% / 50 / 83.6 % after 30 cycles 1227 / 56% / 50 / 79.2 % after 30 cycles	296at 5000 380 at 5000	2
N-doped graphene	70:20:10 AM:CB:PVDF	1 M $LiPF_6$ (EC/DMC)	600 / 67% / 100 / 63% after 50 cycles	201 at 2000	3
Nitrogen-doped carbon xerogels (NCXs)	80:10:10 AM:acetylene black:PVDF	1 M $LiPF_6$ (EC/DMC)	645 / 46% / 37 / N.A	280 at 1860	4
Boron doped graphene (B-G)	75:15:10 AM:PVDF:CB	1M $LiPF_6$ (EC/DMC)	541 / N.A / 50 / 73% after 30 cycles	230 at 1000	5
Boron and nitrogen co-doped porous carbon nanotubes (BN-PCNTs)	85:10:5 AM:CB:PVDF	1 M $LiPF_6$ (EC/DMC)	1261 / 77% / 200 / 71% after 60 cycles	282 at 2000	6
Boron-doped carbon fibers BDCFs	80:10:10 AM:CB:PVDF	1M $LiPF_6$ (EC/DEC)	405 / N.A / 100 / N.A	152 at 1000	7
Nitrogen-doped graphene nanoribbons (N-GNRs)	70:20:10 AM:Acetylene black:PVDF	1M $LiPF_6$ (EC/DEC)	713 / 61% / 100 / 96% after 100 cycles	300 at 3000	8

Graphitized boron-doped carbon foams (B_{GCF})	92:8 AM:PVDF	1M $LiPF_6$ (EC/DEC)	310 / N.A / 37.2 / N.A	N.A	9
Hollow-Structured N-Doped Carbon (HSNC)	90:10 AM:PVDF	1 M $LiPF_6$ (EC/DMC)	1398 / 45% / 200 / 53% after 100 cycles	703 / 1000	10
N-B doped IL based carbon	90:5:5 AM:PVDF:CB	1M $LiPF_6$ (EC/DEC)	250 / 54% / 230 / 98% after 300 cycles	128 / 6900 / 80% after 1400 cycles	This work

Table S4. Elemental composition and carbonization yield of $(Bn)_2$-Cl-P900.

Sample	Elemental composition (wt%)					Mass ratio	C yield (wt%)
	C[a]	H[a]	N[a]	O[a]	Cl[b]	N/C[c]	
$(Bn)_2$-Cl-P900	86.5	1.1	11.7	n/a	0.7	0.14	2.5

[a]Data obtained from combustional elemental analyses. [b]Data extracted from combustional elemental analyses by difference, considering that chlorine is the only element present in addition to carbon, hydrogen, nitrogen and oxygen. [c]Mass ratio calculated from combustional elemental analyses' data.

References:

1 Y. Zhou, Y. Zeng, D. Xu, P. Li, H. Wang, X. Li, Y. Li and Y. Wang, *Electrochimica Acta*, 2015, **184**, 24–31.

2 Z.-S. Wu, W. Ren, L. Xu, F. Li and H.-M. Cheng, *ACS Nano*, 2011, **5**, 5463–5471.

3 Z. Xing, Z. Ju, Y. Zhao, J. Wan, Y. Zhu, Y. Qiang and Y. Qian, *Sci. Rep.*, 2016, **6**, 26146.

4 X. Liu, S. Li, J. Mei, W.-M. Lau, R. Mi, Y. Li, H. Liu and L. Liu, *J Mater Chem A*, 2014, **2**, 14429–14438.

5 M. Sahoo, K. P. Sreena, B. P. Vinayan and S. Ramaprabhu, *Mater. Res. Bull.*, 2015, **61**, 383–390.

6 L. Zhang, G. Xia, Z. Guo, X. Li, D. Sun and X. Yu, *Int. J. Hydrog. Energy*, 2016, **41**, 14252–14260.

7 H. Wang, C. Ma, X. Yang, T. Han, Z. Tao, Y. Song, Z. Liu, Q. Guo and L. Liu, *Solid State Sci.*, 2015, **41**, 36–42.

8 Y. Liu, X. Wang, Y. Dong, Z. Wang, Z. Zhao and J. Qiu, *J Mater Chem A*, 2014, **2**, 16832–16835.

9 E. Rodríguez, I. Cameán, R. García and A. B. García, *Electrochimica Acta*, 2011, **56**, 5090–5094.

10 D.-W. Lee, A. Y. Maulana, C. Lee, J. Song, C. M. Futalan and J. Kim, *Energies*, 2021, **14**, 2436.